Mathematical Modeling of Storm Surge in Three Dimensional Primitive Equations

Worachat Wannawong*, Usa W. Humphries
Prungchan Wongwises and Suphat Vongvisessomjai

Abstract—The mathematical modeling of storm surge in sea and coastal regions such as the South China Sea (SCS) and the Gulf of Thailand (GoT) are important to study the typhoon characteristics. The storm surge causes an inundation at a lateral boundary exhibiting in the coastal zones particularly in the GoT and some part of the SCS. The model simulations in the three dimensional primitive equations with a high resolution model are important to protect local properties and human life from the typhoon surges. In the present study, the mathematical modeling is used to simulate the typhoon–induced surges in three case studies of Typhoon Linda 1997. The results of model simulations at the tide gauge stations can describe the characteristics of storm surges at the coastal zones.

Keywords—lateral boundary, mathematical modeling, numerical simulations, three dimensional primitive equations, storm surge.

I. INTRODUCTION

The numerical experiments of the mathematical modeling are designed to study the storm surges in a three dimensional model. It is important to solve the primitive equations of the surface boundary conditions by the high resolution numerical oceanic model.

The primitive equations are a governing equation of the Princeton Oceanic Model (POM)[1] which is described by the Reynold's averaged equations of mass, momentum, temperature and salinity conservations. The POM model has been developed to study the external gravity waves, internal gravity waves, tidal waves, surges and currents. In 2000, it was applied to study currents in the Gulf of Thailand (GoT) by the Royal Thai Navy. It was also developed by the Thailand Research Fund project in 2003 in order to study the storm–surge and effect of tidal forcing. Wannawong et al. [14] worked on the comparison of orthogonal curvilinear grid and orthogonal rectangular grid in the horizontal coordinates. Even though the velocities of seawater current provided by the orthogonal curvilinear grid were more acceptable in the coastal zone than that of the orthogonal rectangular grid, the velocities of current obtained from both grids were not much different. The orthogonal rectangular grid, therefore, was chosen to study the storm surge and current [14].

Wannawong et al. [15], [16] also studied on the fine grid domain and reported that the storm waves and surges significantly influenced the wave heights and surges [17], [18]. In this study, the numerical ocean predictions were presented

as the time series of the storm surges at ten tide gauge stations by using the three dimensional model. The objective of this work is to modify the mathematical modeling which is the primitive equations under the surface boundary condition of three experiments of the storm surge cases. The study domain is extended from the domain studied by Wannawong et al. [14] to the new domain studied by Wannawong et al. [16], [17] which was similar to the fine grid domain of the storm wave model [18]. Furthermore, the mathematical modeling is modified to study the storm surge cases with the time series of Typhoon Linda 1997 by the POM model. The study domain covering from $99°E$ to $111°E$ in longitude and from $2°N$ to $14°N$ in latitude with high resolution $0.1° \times 0.1°$ is modified to three experiments: 2D–barotropic mode, 3D–baroclinic mode in the prognostic option and 3D–baroclinic mode in the diagnostic option. The experiments are simulated in the study domain by the POM model as illustrated in Fig. 1. The outline of this study is organized as follows: Section II gives a brief description of the three dimensional primitive equations and its modifications to the study domain; Section III presents the model parameters and numerical experiments; Section IV shows the results of experiments; and Section V presents the discussions and also conclusion.

II. THE THREE DIMENSIONAL PRIMITIVE EQUATIONS AND ITS MODIFICATIONS

The mathematical modeling of storm surges used in this study has been modified and described in this section. The three dimensional primitive equations and its modifications were developed from the Princeton Oceanic Model (POM) [1] in order to simulate surges, inundations, currents and coastal circulations. In this section, a brief description of the model applied in the study domain is presented in the following sections.

A. The Three Dimensional Primitive Equations

The governing equation of the three dimensional model can be exhibited in the orthogonal Cartesian coordinate systems which includes the Reynold's averaged equations of mass, momentum, temperature and salinity conservations. The equations not only indicate the effect of the gravitational/buoyancy forces but the effect of the Coriolis pseudo–force is also expressed. The equations can be written as follows.

Continuity equation:

$$\frac{\partial u}{\partial x} + \frac{\partial v}{\partial y} + \frac{\partial w}{\partial z} = 0, \tag{1}$$

x–momentum equation:

$$\frac{du}{dt} = -\frac{1}{\rho_\circ}\frac{\partial p}{\partial x} + fv + \frac{\partial}{\partial z}\left(A_{mv}\frac{\partial u}{\partial z}\right) + F_x, \qquad (2)$$

y–momentum equation:

$$\frac{dv}{dt} = -\frac{1}{\rho_\circ}\frac{\partial p}{\partial y} - fu + \frac{\partial}{\partial z}\left(A_{mv}\frac{\partial v}{\partial z}\right) + F_y, \qquad (3)$$

z–momentum or hydrostatic equation:

$$\frac{\partial p}{\partial z} = -\rho g, \qquad (4)$$

Temperature equation:

$$\frac{dT}{dt} = \frac{\partial}{\partial z}\left(A_{hv}\frac{\partial T}{\partial z}\right) + F_T, \qquad (5)$$

Salinity equation:

$$\frac{dS}{dt} = \frac{\partial}{\partial z}\left(A_{hv}\frac{\partial S}{\partial z}\right) + F_S, \qquad (6)$$

The terms $d(\cdot)/dt$, F_x, F_y, F_T and F_S presented in the equations (2), (3), (5) and (6) represent the total derivative terms, these unresolved processes and in analogy to the molecular diffusion can be described as

$$F_x = \frac{\partial}{\partial x}\left[2A_m\frac{\partial u}{\partial x}\right] + \frac{\partial}{\partial y}\left[A_m\left(\frac{\partial u}{\partial y} + \frac{\partial v}{\partial x}\right)\right],$$

$$F_y = \frac{\partial}{\partial y}\left[2A_m\frac{\partial v}{\partial y}\right] + \frac{\partial}{\partial x}\left[A_m\left(\frac{\partial u}{\partial y} + \frac{\partial v}{\partial x}\right)\right],$$

and

$$F_{T,S} = \frac{\partial}{\partial x}A_h\frac{\partial(T,S)}{\partial x} + \frac{\partial}{\partial y}A_h\frac{\partial(T,S)}{\partial y}.$$

where u, v are the horizontal components of the velocity vector, w is the vertical component of the velocity vector, g is the gravitational acceleration, p is the local pressure, $\rho(x,y,z,t,T,S)$ is the local density, $\rho_\circ$ is the reference water density, A_m is the horizontal turbulent diffusion coefficient, A_{mv} is the vertical turbulent diffusion coefficient, $f = 2\Omega\sin\phi$ is the Coriolis parameter where Ω is the speed of angular rotation of the earth by $\Omega = 7.2921 \times 10^{-5}\ rad\ s^{-1}$ and ϕ is the latitude, T is the potential temperature, S is the potential salinity, A_h is the horizontal thermal diffusivity coefficient, A_{hv} is the vertical thermal diffusivity coefficient, the terms F_x and F_y are the horizontal viscosity terms and the terms F_T and F_S are the horizontal diffusion terms of temperature and salinity respectively.

The main assumptions used in the derivation of above equations are that: (a) the water is incompressible ($d\rho/dt = 0$); (b) the density differences are small and can be neglected, except in buoyant forces (Boussinesq approximation). Consequently, the density $\rho_\circ$ used in the x and y momentum equations (2) and (3) is a reference density that is either represented by the standard density of the water or by the depth averaged water density as follows:

$$\rho_\circ = \frac{1}{\eta + h}\int_{-h}^{\eta}\rho\,dz = \frac{1}{D}\int_{-h}^{\eta}\rho\,dz \qquad (7)$$

where the total depth D is expressed as: $D = \eta + h$ that is, the sum of the sea surface elevation η above the mean sea level (MSL) plus the depth h of the still water level. The density ρ used in the z–momentum is represented by the sum of the reference density $\rho_\circ$ and its variation $\rho'(\rho = \rho_\circ + \rho')$. The last assumption (c) is that, the vertical dimensions are much smaller than the horizontal dimensions of the water field and the vertical motions are much smaller than the horizontal ones. Consequently, the vertical momentum equation reduces to the hydrostatic law (hydrostatic approximation) and the Coriolis term $2\Omega(v\sin\phi - w\cos\phi)$ reduces to $2\Omega v\sin\phi$ (see the equation (2)). The vertical integration of the equation (4) from the depth z to the free surface η yields the pressure at the water depth z as:

$$p|_\eta - p|_z = g\int_z^\eta \rho\,dz' \longrightarrow$$

$$p = p_{atm} + g\rho_\circ(\eta - z) + g\int_z^\eta \rho'\,dz' \qquad (8)$$

where z' is a dummy variable for integration, η is the sea surface elevation above the MSL, $p|_z = p = p(x,y,z,t)$ and $p|_\eta = p_{atm}$ is the standard atmospheric pressure.

It is necessary to state the relationship of the water density, temperature and pressure in order to close the above system of the continuity and motion equations. This relationship in POM model is coded by the following formulation proposed by Mellor [2], that approximates the more general, and also more computationally expensive. The formulations of the International Equation of State (UNESCO) are given below.

$$\rho(S,T,p) = \rho(S,T,0) + \frac{p}{c^2}\left(1 - 0.20\frac{p}{c^2}\right)\cdot 10^4 \qquad (9)$$

$$c(S,T,p) = 1449.2 + 1.34(S - 35) + 4.55T - 0.045T^2$$
$$+ 0.00821p + 15.0\cdot 10^{-9}p^2 \qquad (10)$$

where T is the temperature, p is the gage pressure, S is the salinity and c is the sound speed.

B. Boundary conditions

1) Surface boundary conditions: The continuity, momentum and temperature surface boundary conditions describe the interaction of the water surface with the atmosphere. They are defined as:

$$w|_\eta = \left[\frac{\partial\eta}{\partial t} + u\frac{\partial\eta}{\partial x} + v\frac{\partial\eta}{\partial y}\right]_\eta \qquad (11)$$

$$A_{mv}\begin{bmatrix}\partial u/\partial z \\ \partial v/\partial z\end{bmatrix}_\eta = \begin{bmatrix}\tau_{sx}/\rho_\circ \\ \tau_{sy}/\rho_\circ\end{bmatrix} \qquad (12)$$

$$\dot{T} = \rho_\circ A_{hv}\frac{\partial T}{\partial z}\Big|_\eta \qquad (13)$$

$$\dot{S} = \rho_\circ A_{hv}\frac{\partial S}{\partial z}\Big|_\eta \qquad (14)$$

The equation (11) represents the surface boundary condition for the continuity equation (1), as expressed by the kinematic free surface condition. At free surface, the kinematic boundary condition can be derived considering the fact that the free surface is a material boundary for which a particle initially on the boundary will remain on the boundary. Assuming that

there is no water penetrating the free surface, then the material or total derivative at the free surface $(\eta - z)$ is zero, therefore:

$$\frac{D(\eta - z)}{Dt} = \frac{D\eta}{Dt} - \frac{Dz}{Dt} = 0 \implies$$

$$\left[\frac{\partial \eta}{\partial t} + u\frac{\partial \eta}{\partial x} + v\frac{\partial \eta}{\partial y} + w\frac{\partial \eta}{\partial z}\right]_\eta - \left[\frac{\partial z}{\partial t} + u\frac{\partial z}{\partial x} + v\frac{\partial z}{\partial y}\right.$$

$$\left. + w\frac{\partial z}{\partial z}\right]_z = 0 \quad (15)$$

Since, $\partial \eta/\partial z = \partial z/\partial t = \partial z/\partial x = \partial z/\partial y = 0$ and $\partial z/\partial z = 1$, the equation (15) reduces to the equation (11).

The equation (12) represents the surface boundary condition for the z–momentum or the hydrostatic equation (4) with the surface wind stresses given by the drag law (bulk formula) as:

$$\begin{bmatrix} \tau_{sx} \\ \tau_{sy} \end{bmatrix} = \rho_{air}C_M W \begin{bmatrix} W_x \\ W_y \end{bmatrix} \quad ; \quad \tau_s = \rho_{air}C_M|W|W \quad ;$$

$$W = \left(W_x^2 + W_y^2\right)^{1/2} \quad (16)$$

where W is the wind speed at $10\ m$ above the sea water surface, W_x and W_y are two components of the wind speed vector, ρ_{air} is the density of air at the standard atmospheric conditions, C_M is the bulk momentum transfer (drag) coefficient and τ_s is the wind imposed surface stress.

The drag coefficient (C_M) is assumed to vary with the wind speed as:

$$10^3 C_M = \begin{cases} 2.5 & \text{if } |W| > 22\ m\ s^{-1} \\ 0.49 + 0.065|W| & \text{if } 8 \le |W| \le 22\ m\ s^{-1} \\ 1.2 & \text{if } 4 \le |W| < 8\ m\ s^{-1} \\ 1.1 & \text{if } 1 \le |W| < 4\ m\ s^{-1} \\ 2.6 & \text{if } |W| < 1\ m\ s^{-1} \\ 0.63 + 0.066|W| & \text{for all } |W| \\ 0.63 + (0.066|W|^2)^{1/2} & \text{for all } |W|. \end{cases}$$

This C_M formula follows Large and Pond [13] when the wind speed is less than $22\ m\ s^{-1}$; otherwise, it is assumed to be a constant as indicated in Powell et al. [4]. The equations (13) and (14) represent the surface boundary condition for the temperature and salinity equations (see the equations (15) and (16)). $\dot{T}$ represents the net surface heat flux and $\dot{S} \equiv S(0)[\dot{E} - \dot{P}]/\rho_\circ$ where $(\dot{E} - \dot{P})$ represents the net evaporation $\dot{E}$ – precipitation $\dot{P}$ fresh water surface mass flux rate and $S(0)$ represents the surface salinity.

2) Bottom boundary conditions:

$$w|_{-h} = -\left[u\frac{\partial h}{\partial x} + v\frac{\partial h}{\partial y}\right]_{-h} \quad (17)$$

$$A_{mv}\begin{bmatrix} \partial u/\partial z \\ \partial v/\partial z \end{bmatrix}_{-h} = \begin{bmatrix} \tau_{bx}/\rho_\circ \\ \tau_{by}/\rho_\circ \end{bmatrix} \quad (18)$$

$$\rho_\circ A_{hv}\frac{\partial T}{\partial z}\bigg|_{-h} = 0 \quad (19)$$

$$\rho_\circ A_{hv}\frac{\partial S}{\partial z}\bigg|_{-h} = 0 \quad (20)$$

The equation (17) represents the bottom boundary condition for the continuity equation (1), as expressed by the kinematic

boundary condition. At the bottom, the kinematic boundary condition reflects the fact that there is no flow normal to the boundary, therefore, the material derivative $z + h$ is zero:

$$\frac{D(z + h)}{Dt} = \frac{Dz}{Dt} + \frac{Dh}{Dt} = 0 \implies$$

$$\left[\frac{\partial z}{\partial t} + u\frac{\partial z}{\partial x} + v\frac{\partial z}{\partial y} + w\frac{\partial z}{\partial z}\right]_{-h} + \left[\frac{\partial h}{\partial t} + u\frac{\partial h}{\partial x} + v\frac{\partial h}{\partial y}\right.$$

$$\left. + w\frac{\partial h}{\partial z}\right]_{-h} = 0 \quad (21)$$

and since, $\partial z/\partial t = \partial h/\partial t = \partial z/\partial x = \partial z/\partial y = \partial h/\partial z = 0$ and $\partial z/\partial z = 1$, the equation (21) reduces to the equation (17).

The equation (18) represents the bottom boundary condition for the z–momentum or the hydrostatic equation (4). The bottom shear stresses are parameterized as follows:

$$\begin{bmatrix} \tau_{bx} \\ \tau_{by} \end{bmatrix} = \rho_\circ C_D|u|\begin{bmatrix} u \\ v \end{bmatrix} \quad ; \quad \tau_b = \rho_\circ C_D|u|u \quad ;$$

$$|u| = \left(u^2 + v^2\right)^{1/2} \quad (22)$$

where u and v are the horizontal flow velocities at the grid point closest to bottom and C_D is the bottom drag coefficient determined as the maximum between a value calculated according to the logarithmic law of the wall and a value equal to 0.0025:

$$C_D = \max\left[\mathbf{k}^2\left(\ln\frac{h + z_b}{z_\circ}\right)^{-2}, \ 0.0025\right] \quad (23)$$

where $z_\circ$ is the bottom roughness height in the present application $z_\circ = 1\ cm$, z_b is the grid point closest to bottom, and $\mathbf{k} = 0.4$ is the von Kármán's constant. In the 2D barotropic mode of the POM model, C_D is shown as 0.0025.

On the side walls and bottom of the gulf, the normal gradients of T and S in the equations (19) and (20) are zero. Therefore, there are no advective and diffusive heat and salt fluxes across these boundaries.

3) Lateral boundary conditions: The GoT is modeled as a closed gulf without inflow or outflow from the gulf rivers. Consequently, the lateral conditions for the wall boundary are specified that: (a) there is no flow normal to the wall ($\partial \mathbf{u}_n/\partial n = 0$), and (b) the no slip conditions tangential to the wall are valid ($\mathbf{u}_\tau = 0$), where $\mathbf{u}$ represents the velocity vector, and n and τ are the normal and tangential directions.

C. Wind stress and atmospheric pressure conditions

The typhoon pressure field and surface wind velocity created by the pressure gradient were modeled following the Bowden [3] and Pugh [10] relationships:

$$\frac{\partial p_{air}}{\partial \eta} = -\rho g, \quad (24)$$

$$\frac{\partial \eta}{\partial x} = \frac{\rho_{air}C_M W^2}{\rho g D}. \quad (25)$$

where p_{air} is the atmospheric pressure, η is the sea surface elevation from the reference level of undisturbed surface, ρ

is the density of sea water in the z–momentum, g is the gravitational acceleration of the earth, x is the coordinate in the east–west direction, ρ_{air} is the density of air, C_M is the drag coefficient, W is the wind profile that results from the typhoon pressure gradient and D is the total depth of sea water. According to the equation (24), the pressure reducing for 1 mb corresponds to about a 1 cm rise in the sea level. The total water depth D inversely affects the sea surface elevation η, whereas the wind speed at the specific height (10 m) directly affects the sea surface elevation.

For the POM model, the computational stability condition on the external and internal modes was described by Worachat et al. [16], [17]. The stability of both models was computed according to the Courant–Friedrichs–Lewy (CFL) stability condition. For more details of the sensitivity of the POM model to the time steps, see Ezer et al. [11].

III. THE MODEL PARAMETERS AND NUMERICAL EXPERIMENTS

A. The Bathymetry of the Study Domain

The bathymetry of the study domain is defined by the shoreline, bathymetry and specified transfer boundaries. In some parts of the SCS and GoT, the computations of the model take place on a $0.1° \times 0.1°$ rectangular grid in the horizontal coordinate and on a sigma layer in the vertical coordinate with 21 layers. The domain covered from $99°E$ to $111°E$ in longitude and from $2°N$ to $14°N$ in latitude. The shoreline and bathymetry of the GoT on the $0.1° \times 0.1°$ grid showed in Fig. 1 were obtained from GEODAS (available online from http://www.ngdc.noaa.gov/mgg/gdas). The original version (1993) of ETOPO5 [5], on a 5–minute latitude/longitude grid (1 minute of latitude = 1 nautical mile, or 1.853 km) was updated in June 2005 for the acceptably deep water.

B. Model Initialization and Forcing

The model is initialized by setting the velocity, temperature and salinity fields to be zero. These sets known as "cold start" requires the model run for spin up period before it reaches a state of statistical equilibrium. In the present application, the typhoon spin up period was adequate for the model to reach equilibrium and to provide the realistic results.

The forcing of model during the spin up period and the subsequent model simulations require the use of the following meteorological data: temperature, salinity, sea level pressure, wind speed and direction. The wind and pressure fields were obtained from the U.S. Navy Global Atmospheric Prediction System (NOGAPS) which is a global atmospheric forecasting model with $1° \times 1°$ data resolution (Hogan and Rosmond [12]; Harr et al. [6]). The temperature and salinity with $1° \times 1°$ data resolution provided by Levitus94 (Levitus and Boyer [8]; Levitus et al. [7]) were indicated by the climatological monthly mean fields in the model. The high resolution of $0.1° \times 0.1°$ spatial grid size gave 121×121 points by using the bilinear interpolation of these data in the horizontal coordinate. In the vertical coordinate, 21 sigma levels were employed for adequacy and computational efficiency. The model time steps were 20 s and 1200 s (20 min) for the external and internal time steps respectively.

The horizontal momentum equations consist of the local time derivative and horizontal advection terms, Coriolis deflection, sea level pressure gradient, tangential wind stress on the sea surface, and quadratic bottom friction. The system of equations is written in the flux form and solved by using the finite differential method that is centered in time and space on the Arakawa C grid. Finally, the results of the POM model were correspondingly represented in every hour of Typhoon Linda 1997 entering into some parts of the SCS and GoT. The stability of the model was computed according to the CFL stability condition.

C. Experimental Designs

Three experiments were performed in this study in order to compute the storm surge on the sea surface layer (Table 1). In this study, the storm surge applications of the POM model which is one of the three dimensional model was studied. The POM model was run by considering the difference between 2D and 3D modes with the time series. The model simulations were conducted by using the 2D mode of the POM model as the primary objectives which were to study the barotropic water level variation and volume exchange. To test the adequacy of the POM model, the 2D and 3D modes were tested as described by Blumberg and Mellor [1].

IV. RESULTS OF EXPERIMENTS

The simulations of storm surge were calculated from a set of three dimensional model experiments: Exp. I, Exp. II and Exp. III as described in Table I.

The storm surge generated by Typhoon Linda was firstly considered (Exp. I) and computed by using the POM model as presented in Fig. 4. The Bowden [3] and Pugh [10] relationships were used to describe the storm surges related to the strong wind and low pressure (Figs. (2)–(6)). The POM model using in the three experiments was run with the same wind field (wind speed), pressure field (sea level pressure), domain (wind fetch) and also the same time (duration) but with the different computational options. Fig. (5) illustrated the storm surges at the same location and time with the different optional calculation in Exp. II. In Exp. III (see Fig. (6)), the difference of optional calculation on the sea surface layer can be easily considered in Figs. (4)–(6), which showed that the storm surge increased the setup and slowed down the difference of water recession in 2D and 3D calculations.

The effects of the extreme storm surge and the difference between the maximum storm surges computed by the POM model at ten locations of the tide gauge stations at border of the GoT region (Fig. 1(a) and Table II) were calculated. The differences of storm surges at each station were presented in Table III in [16]. The results showed that the storm surges at each station of all experiments presented the similar values and also expressed the similar trends with the observational data, except for those of the stations S5, S6 and S8 [16], [17]. The time series of the results at ten tide gauge stations of three dimensional model showed in Figs. (7) and (8).

V. Discussions and Conclusion

The comparisons of storm surges on the sea surface layer of the three experiments (Figs. (7) and (8)) in Typhoon Linda cases exhibited that the storm surge played a more significant role in determining the computations for the three dimensional primitive equations by the mathematical modeling (POM model). The role of storm surge without the storm tide under the assumption of negligent tide forcing was presented in this study. The slight differences of storm surges between Exp. I, Exp. II, Exp. III and the observational data of the typhoon distributions during Typhoon Linda entering into the GoT are shown in Figs. (7)–(8).

The results of the model can be considered that the 3D–baroclinic mode increased the setup and slowed down the water recession, thus improving the model performance during the water level declining period while over predicted surge during the water level rising period. Since the specification of the bottom boundary condition depends on the assumption of the vertical velocity profile, the treatments of boundary condition in 2D and 3D modes are not identified, which resulted in the slight different results. The results of this work indicated that the 3D mode did not give the better results compared to the baseline simulation without an additional calibration of the 3D mode case, but the differences are not significant.

For the vertically integrated sea surface elevation calculated by the POM model, the numerical experiments using the storm surge model in the 3D prognostic and 3D diagnostic modes have been performed. In the prognostic mode, the momentum equations as well as the temperature and salinity distributions of the governing equation were integrated as an initial condition. These predictive experiments do not always reach the steady state due to the oceanic response time for the density field can be considerable. As an alternative, diagnostic computation was considered. Additional studies will be investigated in the future with a focus on how storm surges affect other domains in the GoT. The effects of the storm surge on the sea surface layer should be more comprehensively examined with more typhoon case simulations. Additionally, the calibration and validation of the observational data with the harmonic analysis of tide in other models are needed [9].

Acknowledgments

References

[1] A. F. Blumberg and G. L. Mellor, A description of a three–dimensional coastal ocean circulation model, In N. S. Heaps, editor, Three–Dimensional Coastal Ocean Models, Coastal and Estuarine Sciences, American Geophysical Union, Washington, DC, 4(1987), 1–16.

[2] G. L. Mellor, An equation of state for numerical models of oceans and estuaries, Journal of Atmospheric and Oceanic Technology, 8(1991), 609–611.

[3] K. F. Bowden, Physical oceanography of coastal waters, Ellis Horwood, Southampton, UK., (1983), 302.

[4] M. D. Powell, P. J. Vivkery and T. A. Reinhold, Reduced drag coefficient for high wind speeds in tropical cyclones, Nature, 422(2003), 278–283.

[5] M. O. Edwards, Global Gridded Elevation and Bathymetry on 5–Minute Geographic Grid (ETOPO5), NOAA, National Geophysical Data Center, Boulder, Colorado, U.S.A., 1989.

[6] P. Harr, R. Ellsberry, T. Hogan and W. Clune, North Pacific cyclone sea–level pressure errors with NOGAPS, Weather and Forecasting, 7(1992), 3.

[7] S. Levitus, R. Burgett and T. Boyer, World Ocean Atlas: Salinity, NOAA Atlas NESDIS 3, U. S. Government Printing Office, Washington D.C., U.S.A., 3(1994b), 99.

[8] S. Levitus and T. Boyer, World Ocean Atlas: Temperature, NOAA Atlas NESDIS 4, U. S. Government Printing Office, Washington D.C., U.S.A., 4(1994a), 117.

[9] S. Vongvisessomjai, P. Chatanantavet and P. Srivihok, Interaction of tide and salinity barrier: Limitation of numerical model, Songklanakarin Journal of Science and Technology, 30(2008), 531–538.

[10] T. D. Pugh, Tides, Surges and Mean Sea–Level, John Wiley & Sons, London, UK., (1987), 472.

[11] T. Ezer, H. Arango and A. F. Shchepetkin, Developments in terrain–following ocean models: intercomparison of numerical aspects, Ocean Modelling, 4(2002), 249–267.

[12] T. F. Hogan and T. E. Rosmond, The description of the Navy Operational Global Atmospheric System's spectral forecast model, Monthly Weather Review, 119(1991), 1786–1815.

[13] W. G. Large and S. Pond, Open ocean momentum fluxes in moderate to strong winds, Journal of Physical Oceanography, 11(1981), 324–336.

[14] W. Wannawong, U. W. Humphries and A. Luadsong, The application of curvilinear coordinate for primitive equation in the Gulf of Thailand, Thai Journal of Mathematics, 6(2008), 89–108.

[15] W. Wannawong, U. W. Humphries, P. Wongwises, S. Vongvisessomjai and W. Lueangaram, A numerical study of two coordinates for energy balance equations by wave model, Thai Journal of Mathematics, 8(2010), 197–214.

[16] W. Wannawong, U. W. Humphries, P. Wongwises, S. Vongvisessomjai and W. Lueangaram, Numerical modeling and computation of storm surge for primitive equation by hydrodynamic model, Thai Journal of Mathematics, 8(2010), 347–363.

[17] W. Wannawong, U. W. Humphries, P. Wongwises, S. Vongvisessomjai and W. Lueangaram, Numerical analysis of wave and hydrodynamic models for energy balance and primitive equations, International Journal of Mathematical and Statistical Sciences, 4(2010), 140–150.

[18] W. Wannawong, U. W. Humphries, P. Wongwises and S. Vongvisessom-jai, Three steps of one–way nested grid for energy balance equations by wave model, International Journal of Computational and Mathematical Sciences, 1(2011), 23–30.

Worachat Wannawong received the B.Sc. degree in science–physics from Srinakharinwirot University, Bangkok, Thailand, in 2003, and the M.Sc. and Ph.D. degrees in applied mathematics from King Mongkut's University of Technology Thonburi (KMUTT), Bangkok, Thailand, in 2006 and 2010, respectively. He was with the Numerical Weather Prediction Center, Hydrographic Department, Royal Thai Navy from 2008 to 2010. He joined the Regional Ocean Modeling System (ROMS) team in October 2008. In April 2009, a part of his work was advised by Prof. Charitha Pattiaratchi and Prof. Krish Thiagarajan from the School of Environmental Systems Engineering and the School of Mechanical Engineering, University of Western Australia. In December 2009, he joined the workshop of the climate change project at KMUTT and Prof. Zhu Jiang from the Institute of Atmospheric Physics (IAP), Chinese Academy of Sciences, Beijing University gave him many ideas to modify the storm surge model by adjusting the drag coefficient. His research interests involve numerical analysis, numerical weather prediction, computational mathematics, and mathematical modeling.
Email: worachataj@hotmail.com

Prungchan Wongwises received the B.Sc. (Second Honor) degree in mathematics from Chulalongkorn University, Bangkok, Thailand, in 1962, and the Diplom. Math. and Dr.rer.nat. degrees in mathematics from Technical University of Karlsruhe, Germany, in 1969 and 1974, respectively. She got the scholarships from the Technical University of Karlsruhe (Deutscher Akademischer Austauschdienst, DAAD), University of Freiburg, University of Kassel and University of Hannover under the German Government from 1966 to 1993. She currently is an Associate Professor with the Joint Graduate School of Energy and Environment, KMUTT. Her research interests include numerical analysis, computational mathematics, atmospheric modeling, oceanic modeling and air pollution modeling.
Email: prungchan.won@kmutt.ac.th

Usa W. Humphries received the B.Sc. degree in mathematics from Prince of Songkla University, Songkla, Thailand, in 1991, the M.Sc. degree in applied mathematics from KMUTT, in 1994, and the Ph.D. degree in applied mathematics from University of Exeter, England, in 2000. She was a National Research Council Postdoctoral Investigator with the James Rennell Division University of Southampton, Southampton, England, from November 2001 to December 2002 and with the IAP, China, from October 10 to November 10, 2005. She currently is an Associate Professor with the Department of Mathematics, KMUTT. Her research interests include numerical analysis, computational mathematics, oceanic modeling and climate change.
Email: usa.wan@kmutt.ac.th

Suphat Vongvisessomjai is a Professor of Hydraulic and Coastal Engineering with the Water and Environment Expert, TEAM Consulting Engineering and Management Co., Ltd., Thailand. He was a lecturer in the Division of Water Resources Engineering, Asian Institute of Technology (AIT), Thailand, from 1968 to present and a project engineer in the Delft Hydraulics Laboratory, Netherlands, in 1980. He currently is a Professor and Director of Regional Environmental Management Center, Thailand. His research interests include drainage and flood control, coastal erosion and pollution, and water resources.
Email: suphat@team.co.th

Experimental code	Description of numerical experiments
Exp.I	2D–barotropic mode
Exp.II	3D–baroclinic mode in the prognostic option
Exp.III	3D–baroclinic mode in the diagnostic option

TABLE II
THE COMPUTATIONAL AND OBSERVATIONAL POINTS FOR THE THREE
DIMENSIONAL MODEL SIMULATIONS

Station code	Station name	Station point	Computational point
S1	Laem Ngob	$102.40° E$ $12.10° N$	$102.38° E$ $12.08° N$
S2	Laem Sing	$102.07° E$ $12.47° N$	$102.05° E$ $12.47° N$
S3	Prasae	$101.70° E$ $12.70° N$	$101.70° E$ $12.68° N$
S4	Rayong	$101.28° E$ $12.67° N$	$101.28° E$ $12.65° N$
S5	Tha Chin	$100.28° E$ $13.48° N$	$100.28° E$ $13.45° N$
S6	Mae Klong	$100.00° E$ $13.38° N$	$100.03° E$ $13.35° N$
S7	Pranburi	$99.98° E$ $12.40° N$	$100.10° E$ $12.40° N$
S8	Hua Hin	$99.97° E$ $12.57° N$	$99.95° E$ $12.57° N$
S9	Ko Lak	$99.82° E$ $11.80° N$	$99.84° E$ $11.78° N$
S10	Sichol	$99.90° E$ $9.00° N$	$99.92° E$ $8.98° N$
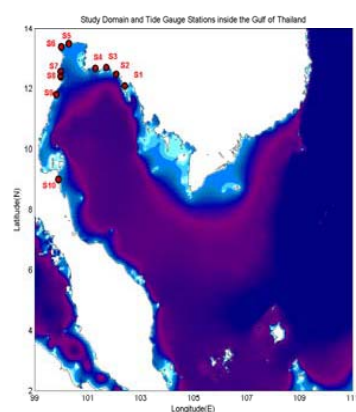
(a) Ten tide gauge stations at border of the GoT
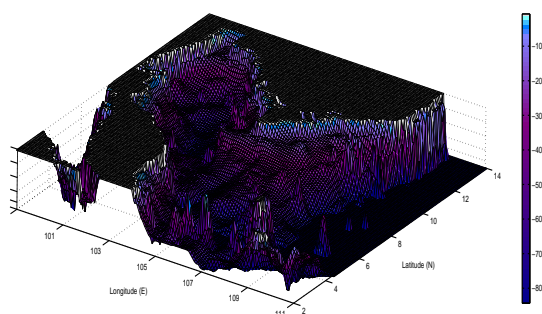
(b) Bathymetry in the perspective view

Fig. 1. (a) The study domain and observational points, and (b) the three dimensional bathymetry (m) in the perspective view
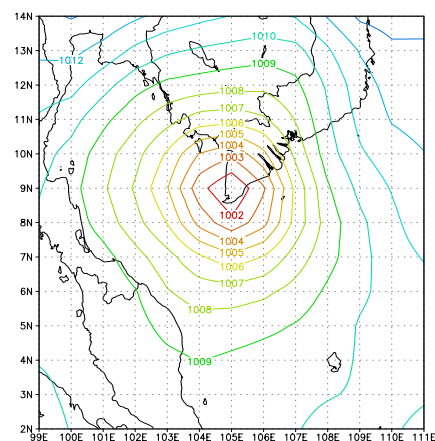
(a) 12UTC02NOV1997
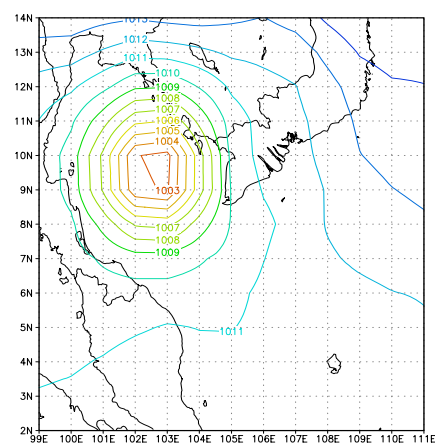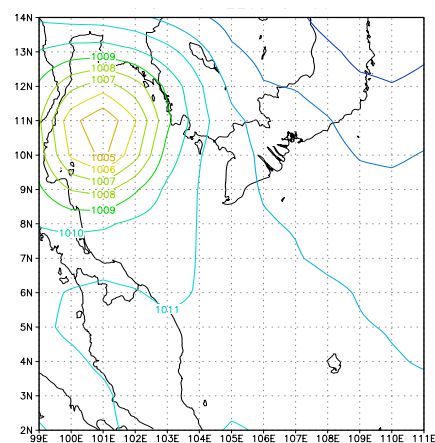
(b) 00UTC03NOV1997

(c) 12UTC03NOV1997

Fig. 2. Sea level pressures (hPa) at the sea surface layer before and after entering into the GoT
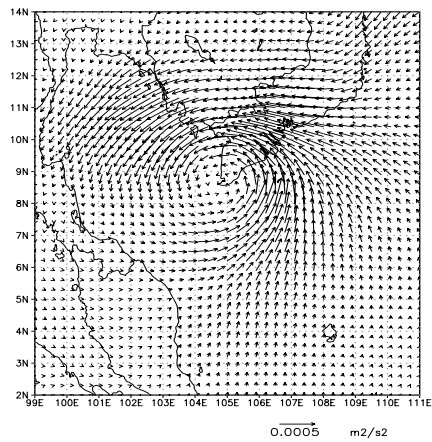
(a) 12UTC02NOV1997
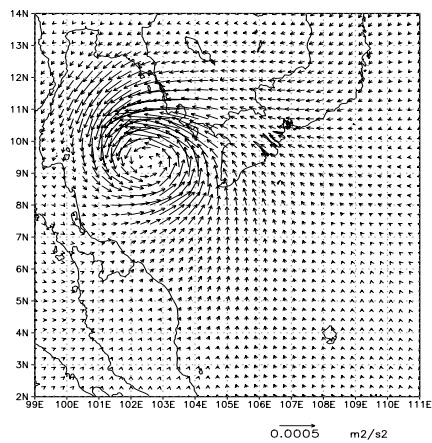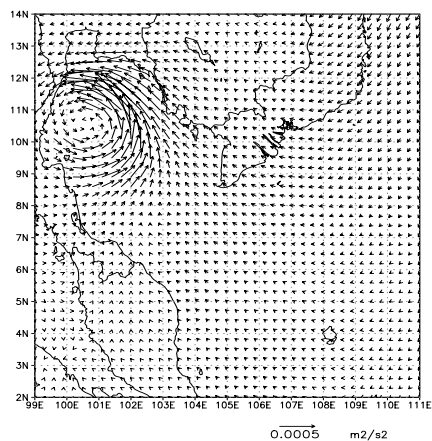
(b) 00UTC03NOV1997

(c) 12UTC03NOV1997

Fig. 3. Wind stress and its direction before and after entering into the GoT
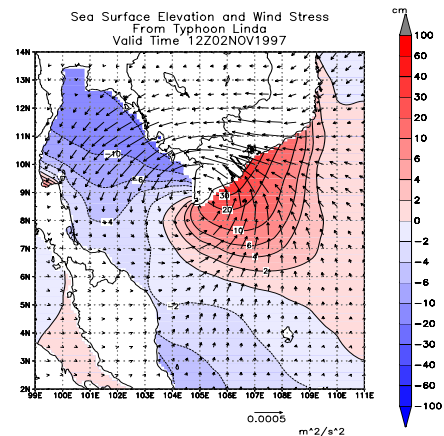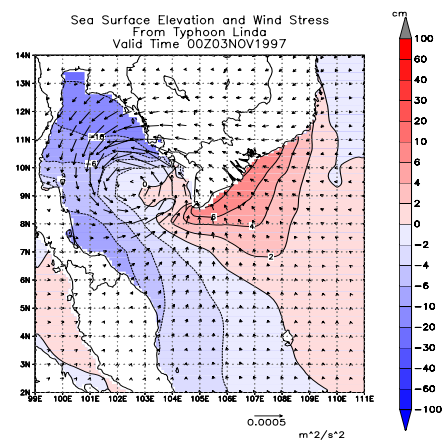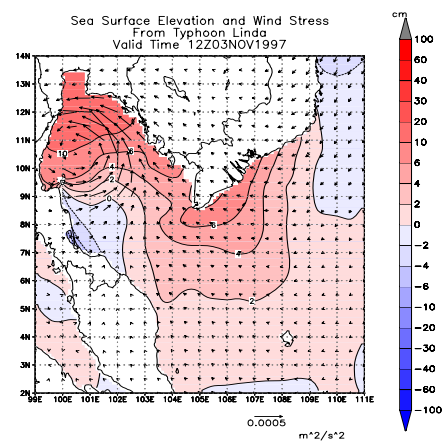
(a) Before

(b) After

(c) Nearshore

Fig. 4. Sea surface elevation and wind stress in the 2D–barotropic mode before and after entering into the GoT
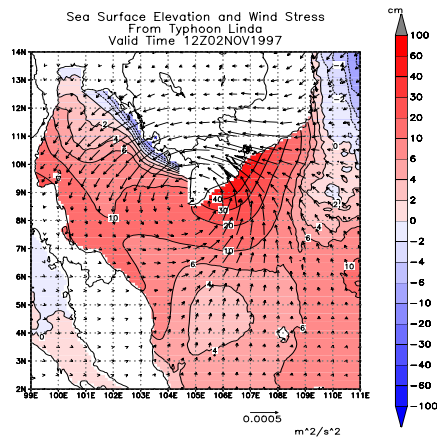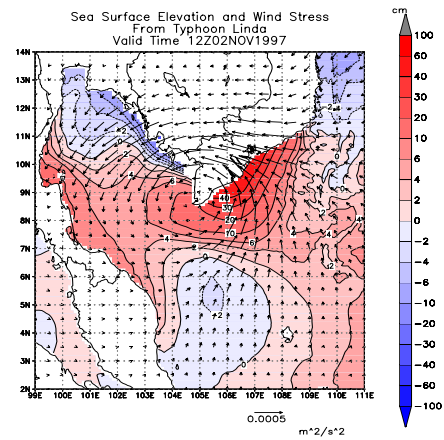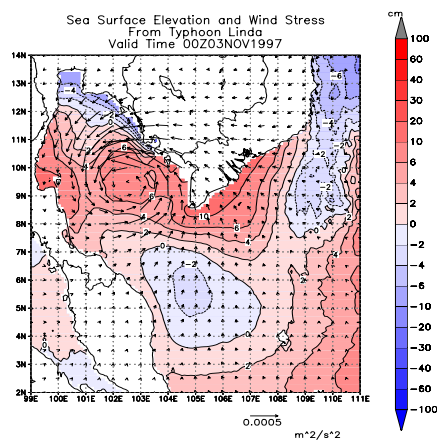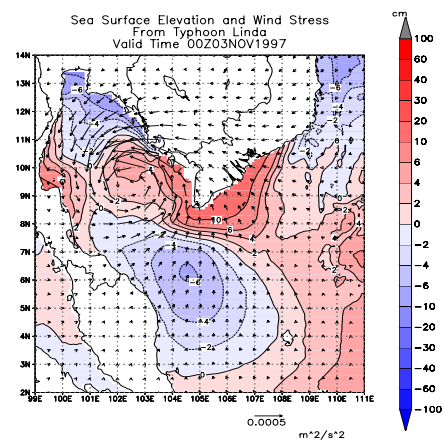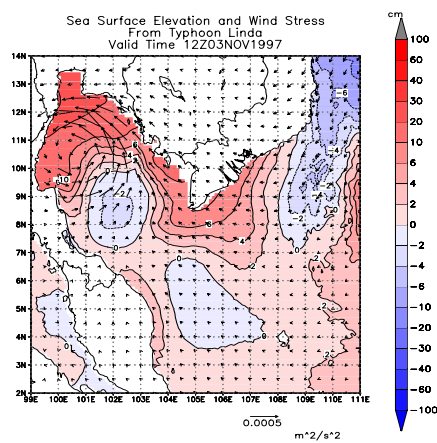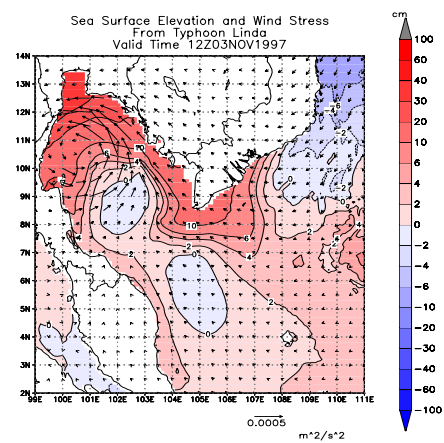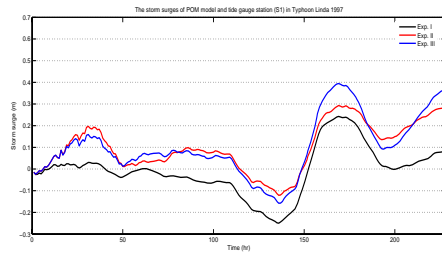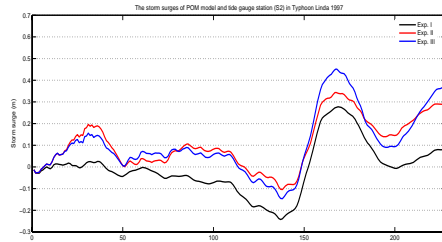
(a) Before

(b) After

(c) Nearshore

Fig. 5. Sea surface elevation and wind stress in the 3D–baroclinic mode with the prognostic option before and after entering into the GoT
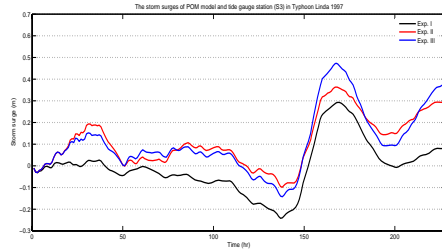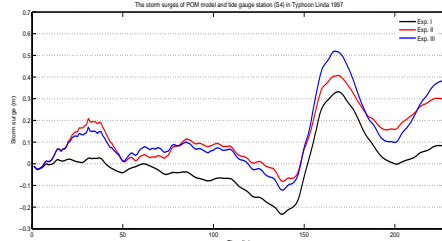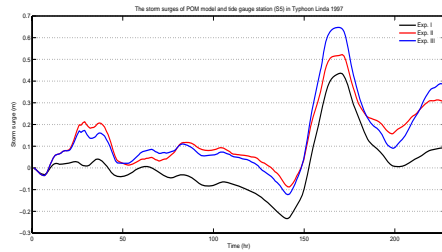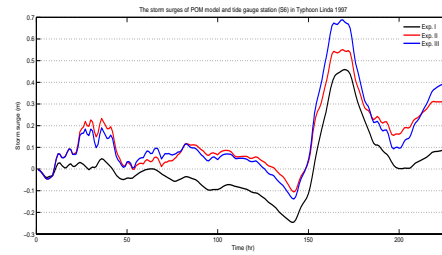

(a) Before

(b) After

(c) Nearshore

Fig. 6. Sea surface elevation and wind stress in the 3D–baroclinic mode with the diagnostic option before and after entering into the GoT
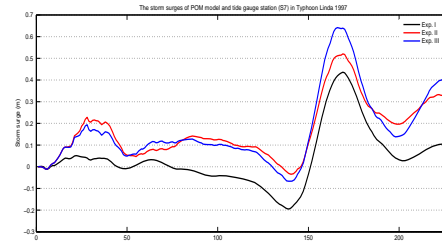
(a) S1

(b) S2

(c) S3

(d) S4

(e) S5
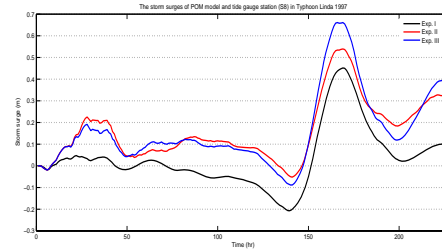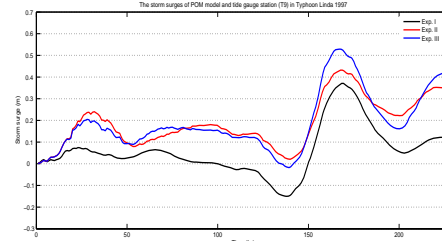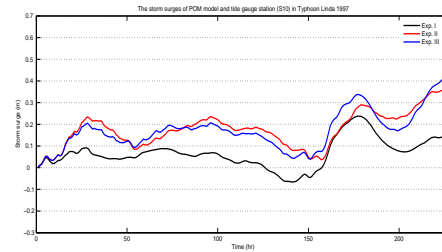
Fig. 7. Comparison of three experiments at five tide gauge stations from S1 to S5

(a) S6

(b) S7

(c) S8

(d) S9

(e) S10

Fig. 8. Comparison of three experiments at five tide gauge stations from S6 to S10